Field Diffusion Equation in High-Speed Surface Mounted Permanent Magnet Motors, Parasitic Eddy-Current Losses

Frédéric Dubas, Christophe Espanet, A. Miraoui

6th International Symposium on Advanced Electromechanical Motion Systems
ELECTROMOTION 2005
LAUSANNE, SWITZERLAND
September 27-29, 2005

FIELD DIFFUSION EQUATION IN HIGH-SPEED SURFACE-MOUNTED PERMANENT MAGNET MOTORS, PARASITIC EDDY-CURRENT LOSSES

F. Dubas, C. Espanet and A. Miraoui

Electrical Engineering and Systems Laboratory (L2ES).
Joint Research Unit of the University of Technology of Belfort-Montbéliard (UTBM)
and the University of Franche-Comté (UFC) – EA 3898
Rue Thierry Mieg, F-90010 Belfort, France

Abstract — The authors present a general computation of the time-varying magnetic flux density distribution of high-speed surface mounted permanent magnet (PM) motors (SMPMM). It deals with an analytical model (AM) which is based on a two-dimensional (2-D) analysis in polar co-ordinates and solves the governing Helmholtz/Laplace field equation in the air-gap/magnet/rotor yoke regions, with due account of the eddy-current reaction field. It enables the parasitic eddy-current losses in the turning parts (i.e. PM and rotor yoke) to be calculated for SMPMM, having either internal or external rotor topologies and overlapping stator windings. This analysis accounts for both time and space magnetomotive force (MMF) harmonics, but neglects the influence of the stator slotting. The analytical results are compared with the ones obtained by numerical analysis using the finite-element method (FEM) and show a good agreement.

1. INTRODUCTION

High-speed brushless permanent magnet (PM) motors with surface-mounted PM are likely to be a key technology for many future applications of motion control and drives systems, since they lead to high efficiency, small size and light weight [1]. In order to maintain the mechanical integrity of a PM machine rotor intended for high-speed operation, the rotor assembly is often retained within a retaining sleeve, which may be either conducting or non-conducting [2]. In these types of machines, the conducting retaining sleeve, the PM, and the rotor back-iron are exposed to high order flux harmonics which are not synchronous with the rotor. The parasitic eddy-current losses, caused by these non-synchronous fields, are a well known problem in conventional synchronous machine design. More specifically, the losses in the turning parts result from both stator slotting permeance harmonics [3-5] and MMF harmonics which are of two types: **(a)** MMF harmonics caused by the discrete positions of stator winding conductors [6-8], and **(b)** MMF harmonics caused by time harmonics in the stator current, which result from six-step commutation [9-11] and Pulse-Width-Modulation (PWM) [12].

Most of the time, the parasitic eddy-current losses tend to negligible for small actuator motors and low speed machines, but are of considerable amount in large machines used, e.g., in electric and hybrid propulsion systems. Hence, the ability to predict these losses is very important for the machine designers in order to evaluate the loss effect on the temperature rise and to avoid thermal stress and magnet damage.

A full study of the magnetic fields and induced eddy-currents can be made using time stepping finite-element analysis [4, 6]. But these techniques are very time consuming – due to the combination of magnetic non linearity and the requirement to model the relative movement of the rotor and stator – and, therefore, not suitable for design studies and optimization. Further, since the induced eddy-currents can be highly not uniformly distributed, a fine discretisation may be necessary to accurately model skin effect, which, in turn, may give rise to numerical instability issues. Then, the AM are often preferred for predicting the eddy-current losses in the turning parts at the design stage. It is thus necessary to solve the diffusion equation [3, 5, 9-12] in order to take into account the influence of the eddy-current reaction field.

In order to satisfy the continuing request for improving the design's precision and generality, the authors have developed a 2-D polar co-ordinate AM for calculating the eddy-current losses in the turning parts of high-speed SMPMM, with a non-conducting retaining sleeve, having either internal or external rotor topologies and overlapping stator windings. It involves resolution of Helmholtz/Laplace's equations in the air-gap/PM/rotor yoke regions using the complex Fourier's series and the method of separating variables. The main originality of this AM that it makes it possible to predict the time-varying magnetic flux density in rotor steel, contrary for example to the AM is presented in [11]. As in [9-12], the method is general because it accounts for curvature, time and space MMF harmonics, and effect of the eddy-current reaction field. However, as in [11], it neglects the air-gap permeance variation due to stator slotting. With these assumptions, the influence of the eddy-currents on the inducing field and the losses in the turning parts are clarified. For a given machine the evolution of these losses versus the rotational speed is given. Finally, the

analytical results are compared with the ones obtained by numerical analysis using the FEM [13].

2. MATHEMATICAL APPROACH

A. Problem Description and Simplifying Assumptions

The SMPMM for both internal and external rotor topologies and the parameters of these geometries are presented in Fig. 1.a. The main assumptions are: **1)** End effects are ignored; **2)** The PM with $\alpha_p = 1$ and the rotor yoke are homogeneous, isotropic, and characterized by the constant relative magnetic permeabilities, μ_{rII} and μ_{rIII}, and constant electrical conductivities, σ_{II} and σ_{III}; **3)** The permeability of stator laminations is assumed to be infinite, thus there are no eddy-current losses in the stator; **4)** The saturation effects of the armatures are neglected; **5)** The permeance variation due to stator slotting is neglected; and **6)** The stator winding is represented by an equivalent linear distribution over the stator slot openings.

B. Slotted Stator Modification

For Brushless PM machines with a slotted stator, the effect of slotting may taken into account by introducing a Carter's coefficient K_c. In fact, the slotted stator is transformed into a slotless stator (see Fig. 1.b.) by applying this coefficient which is approximated by [15]

$$K_c = \tau_t / \left(\tau_t - \gamma \cdot g_{ext}\right), \tag{1}$$

where τ_t is the stator tooth-pitch; $g_{ext} = g + h_m/\mu_{rm}$; g is the actual air-gap length; μ_{rm} is the relative magnetic permeability of the PM and h_m is their radial thickness; and the slot-width reduction factor γ is given by

$$\gamma = 4 \cdot \left[\beta \cdot \tan^{-1}(\beta) - \ln\sqrt{1+\beta^2}\right] / \pi, \tag{2}$$

where $\beta = b_0/(2g_{ext})$; b_0 is the width of the stator slot opening.
Therefore, the effective air-gap g' and the equivalent armature bore radius R'_s are given, respectively, by

$$g' = g + (K_c - 1) \cdot g_{ext}, \tag{3.a}$$
$$R'_s = R_s + k_s \cdot (K_c - 1) \cdot g_{ext}, \tag{3.b}$$

where R_s is the radius of the stator surface adjacent to air-gap, and k_s is the index of motor topologies ($k_s = 1$: internal rotor or $k_s = -1$: external rotor).

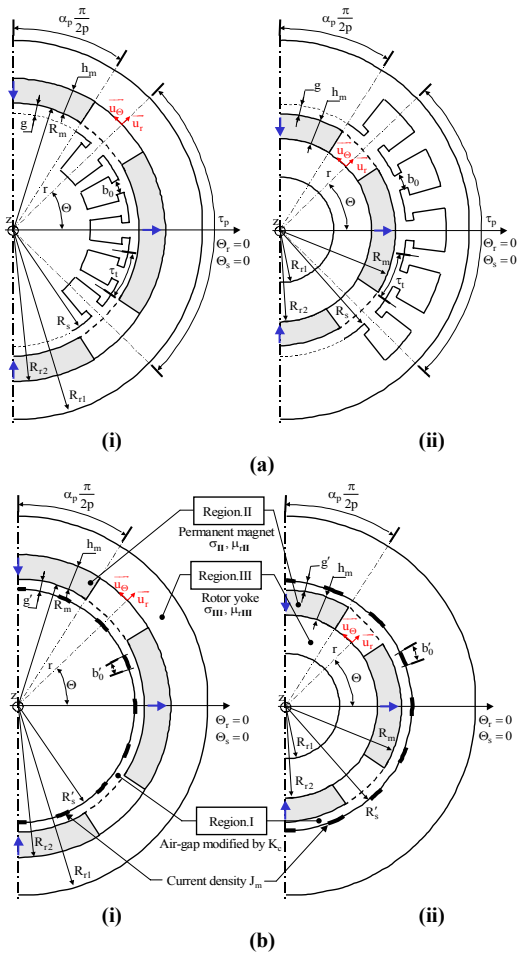

Fig. 1. Motor topologies **(a)** real **(b)** simplified with a **(i)** external or **(ii)** internal rotor.

C. Stator Excitation Functions

In a Brushless PM machine, the phase winding current waveform (for 180°*e* squarewave conducting mode), which may be either analytical or numerical, contains significant harmonics. These can be expressed as a complex Fourier series, as following:

$$i_g(t) = \Re e\left\{\sum_{u=-\infty}^{+\infty} I_u \cdot e^{j \cdot u \cdot \left(\omega_0 \cdot t - \varphi - g \cdot \frac{2\pi}{m}\right)}\right\}, \tag{4}$$

where g is the index of phases (*A*: 0, *B*: 1, and *C*: 2); u is the time harmonic orders ($u \neq 0$ and odd); I_u is the stator harmonic current of order u; $j = \sqrt{-1}$; ω_0 is the rotor angular velocity (electrical); t is the time; φ is the phase displacement of the current in relation to the voltage; and m is the number of phases.
The stator resultant MMF waveforms produced by the overlapping *m*-phases stator windings, derived from an analytical prediction of the current waveform, can be obtained by applying complex Fourier analysis:

$$F_m(t,\Theta_s)=\Re e\left\{\sum_{u=-\infty}^{+\infty}\sum_{v=-\infty}^{+\infty}\underline{F_m}_{uv}\cdot e^{j\cdot\left[f_{uv}(t)+vp\cdot\Theta_s\right]}\right\}, \quad (5)$$

where $f_{uv}(t,\Theta_s)=u\cdot(\omega_0\cdot t-\varphi)$; v is the spatial harmonic orders ($v\neq 0$ and odd); p is the number of pole pairs; Θ_s is the mechanical angular position of the stator (the position $\Theta_s=0$ is defined in Fig. 1); and $\underline{F_m}_{uv}$ represents the complex harmonic amplitude of MMF which is defined by:

$$\underline{F_m}_{uv}=I_u\cdot\underline{F_m}_v=\begin{cases}-j\cdot m\cdot\dfrac{N\alpha_0}{\pi}\cdot I_u\cdot K_{wf_v} & \text{for } |u+v|=m\cdot s\\ 0 & \text{for } |u+v|\neq m\cdot s\end{cases}, \quad (6)$$

where $s=0,1,...,+\infty$; N is the number of series turns per phase; $\alpha_0=b_0/R_s$; and $K_{wf_v}=K_{sof_v}\cdot K_{wof_v}\cdot K_{wdf_v}\cdot K_{itf_v}$ is the winding factor with [14]:

- K_{sof_v} is the slot-opening factor:

$$K_{sof_v}=\sin\left(vp\cdot\frac{\alpha_0}{2}\right)\Big/\left(vp\cdot\frac{\alpha_0}{2}\right), \quad (7.a)$$

- $K_{tpf_v}(x)$ is the stator tooth-pitch factor:

$$K_{tpf_v}(x)=\sin\left(x\cdot vp\cdot\frac{\alpha_t}{2}\right)\Big/\left(x\cdot vp\cdot\frac{\alpha_t}{2}\right), \quad (7.b)$$

- K_{wof_v} is the winding opening factor:

$$K_{wof_v}=\sin\left(vp\cdot\frac{\tau_p}{2}\right)\cdot\cos\left(N_1\cdot vp\cdot\frac{\alpha_t}{2}\right)\cdot\frac{K_{tpf_v}(N_c\cdot N_2)}{K_{tpf_v}(N_2)}, \quad (7.c)$$

- K_{wdf_v} is the winding distribution factor:

$$K_{wdf_v}=K_{tpf_v}(q)\big/K_{tpf_v}(1), \quad (7.d)$$

- K_{tif_v} is the tooth inclination factor:

$$K_{tif_v}=K_{tpf_v}(y_i), \quad (7.e)$$

where τ_p is the pole-pitch; $\alpha_t=\tau_t/R_s=2\pi/Q_s$; $Q_s=2p\cdot m\cdot q$ is the total number of slots; q is the number of stator slots per pole per phase; N_c is the number of layers; y_i is the span of tooth inclination; $N_1=m\cdot q-N_1'$; N_1' is the number of slots between two serial consecutive conductors in the first layer; and N_2 is the number of slots between two consecutive layers. The ratio of τ_{cp}/τ_p, with τ_{cp} the coil span, permit to define the winding pitch

$$y_{wp}=\left[1-(N_1+N_2)\cdot\alpha_t/\tau_p\right]. \quad (8)$$

By dividing equation (5) by $b_0'=\alpha_0\cdot R_s'$ the width of the stator slot opening modified by K_c, the equivalent current density distribution at the stator surface can be written as:

$$J_m(t,\Theta_s)=\Re e\left\{\sum_{u=-\infty}^{+\infty}\sum_{v=-\infty}^{+\infty}\underline{J_m}_{uv}\cdot e^{j\cdot\left[f_{uv}(t)+vp\cdot\Theta_s\right]}\right\}. \quad (9)$$

D. General Differential Equations in Polar Coordinates

By assuming that the term $\partial\vec{D}/\partial t$ is negligible in comparison with the conduction current density $\vec{J}$, the Maxwell's equations are written, as following:

$$\overrightarrow{rot}\left(\vec{E}\right)=-\frac{\partial\vec{B}}{\partial t} \quad \textit{Faraday's law}, \quad (10.a)$$

$$div\left(\vec{B}\right)=0 \quad \textit{Magnetic flux conservation}, \quad (10.b)$$

$$div\left(\vec{J}\right)=0 \quad \textit{Electric charge conservation}, \quad (10.c)$$

$$rot\left(\vec{H}\right)=\vec{J} \quad \textit{Ampere's law}, \quad (10.d)$$

$$\vec{B}=\mu\cdot\vec{H}+\vec{B_r} \quad \textit{Magnetic material equation}, \quad (10.e)$$

$$\vec{J}=\sigma\cdot\vec{E} \quad \textit{Ohm's law}, \quad (10.f)$$

where $\vec{E}$ is the electric field vector; $\vec{B}$ is the magnetic flux density vector; $\vec{J}$ is the eddy-current density vector; $\vec{H}$ is the magnetic field vector; $\mu=\mu_0\cdot\mu_r$; μ_0 is the permeability of free space, μ_r and σ are the relative magnetic permeability and the electrical conductivity of the material. The magnetic vector potential $\vec{A}$ is defined by

$$\vec{B}=\overrightarrow{rot}\left(\vec{A}\right) \text{ with } div\left(\vec{A}\right)=0 \quad \textit{Coulomb's gage}. \quad (10.g)$$

In order to obtain the time-varying armature reaction magnetic flux density distribution and the associated losses in the turning parts due to $J_m(t,\Theta_s)$ at the stator surface, it is necessary to solve the diffusion equation in the rotating reference frame Θ_r (the position $\Theta_r=0$ is in the center of a North magnet, see Fig 1). The domain of study consists of three concentric regions (see Fig. 1.b.), of constant thickness and permeabilitie, namely the air-gap modified by K_c (Region.I), the PM (Region.II), and the rotor yoke (Region.III). Using equations (10), and

neglecting the end effects ($\overrightarrow{A_{ri}} = A_{ri}^{z} \cdot \overrightarrow{u_z}$ and $\vec{J} = J^{z} \cdot \overrightarrow{u_z}$), the time-varying armature reaction magnetic vector potential verifies the Laplace's equation in Region.I

$$\Delta A_{\mathbf{I}ri}^{z}\left(t,r,\Theta_r\right) = 0\,, \tag{11.a}$$

and the Helmholtz's equation in Region.II/III

$$\Delta A_{\mathbf{k}ri}^{z}\left(t,r,\Theta_r\right) - A_{\mathbf{k}ri}^{z}\left(t,r,\Theta_r\right) \Big/ \underline{\delta_{\mathbf{k}}}_{uv}^{\,2} = 0\,, \tag{11.b}$$

where $\mathbf{k}$ is the index of conducting regions (**II**: Region.II, and **III**: Region.III), and $\underline{\delta_{\mathbf{k}}}_{uv}$ represents the complex skin depth of the conducting regions which is defined by

$$\underline{\delta_{\mathbf{k}}}_{uv} = \frac{\underline{\alpha_{\mathbf{k}}}_{uv}}{1+j} = \frac{1}{1+j} \cdot \sqrt{\frac{2}{(u+v)\cdot\sigma_{\mathbf{k}}\cdot\mu_{\mathbf{k}}\cdot\omega_0}}\,, \tag{12}$$

E. General Solutions In Polar Coordinates

Assuming that the stator iron is infinitely permeable, the boundary condictions at the interface between the different regions, ($\forall t$ and Θ_r), are defined by

$$B_{\mathbf{I}ri}^{\Theta}\left(t,R_s',\Theta_r\right) = -k_s\cdot\mu_0\cdot J_m\left(t,\Theta_r\right), \tag{13.a}$$
$$B_{\mathbf{I}ri}^{\Theta}\left(t,R_m,\Theta_r\right) = \nu_{rII}\cdot B_{\mathbf{II}ri}^{\Theta}\left(t,R_m,\Theta_r\right), \tag{13.b}$$
$$B_{\mathbf{I}ri}^{r}\left(t,R_m,\Theta_r\right) = B_{\mathbf{II}ri}^{r}\left(t,R_m,\Theta_r\right), \tag{13.c}$$
$$\nu_{rII}\cdot B_{\mathbf{II}ri}^{\Theta}\left(t,R_{r2},\Theta_r\right) = \nu_{rIII}\cdot B_{\mathbf{III}ri}^{\Theta}\left(t,R_{r2},\Theta_r\right), \tag{13.d}$$
$$B_{\mathbf{II}ri}^{r}\left(t,R_{r2},\Theta_r\right) = B_{\mathbf{III}ri}^{r}\left(t,R_{r2},\Theta_r\right), \tag{13.e}$$
$$B_{\mathbf{III}ri}^{r}\left(t,R_{r1},\Theta_r\right) = 0\,, \tag{13.f}$$

where $\nu_{r\mathbf{k}} = 1/\mu_{r\mathbf{k}}$ is the relative magnetic reluctivity of conducting regions.

By using the method of separating variables and by solving the equations (11) with the equations (13), the complex Fourier's series of the armature reaction vector magnetic potential can be obtained. In each region, the equation (10.g) gives the radial and tangential components of the time-varying armature reaction magnetic flux density vector in complex Fourier series:

$$B_{\mathbf{j}ri}^{r/\Theta}\left(t,r,\Theta_r\right) = \Re_e\left\{\sum_{u=-\infty}^{+\infty}\sum_{v=-\infty}^{+\infty} \underline{B_{\mathbf{j}ri}^{r/\Theta}}_{uv}\left(r\right)\cdot e^{j\cdot\left[g_{uv}(t)+vp\cdot\Theta_r\right]}\right\}, \tag{14}$$

where $g_{uv}\left(t\right) = \left(u+v\right)\cdot\left(\omega_0\cdot t-\varphi\right)+v\cdot\left(\psi-\pi/2\right)$; **j** is the index of the region (**I**: Region.I, **II**: Region.II, and **III**: Region.III); ψ is the phase displacement of the current in relation to the electromotive force (EMF); and $\underline{B_{\mathbf{j}ri}^{r/\Theta}}_{uv}\left(r\right)$ represents the various harmonic amplitudes of the radial and tangential components for the $B_{\mathbf{j}ri}^{r/\Theta}\left(t,r,\Theta_r\right)$ which are given in the Tab. I. We can notice that these amplitudes depend mainly on u, v, p, $\underline{J_m}_{uv}$, k_s, the various adimensional ratios of regions (see Tab. I), and the modified Bessel functions of the first and second kinds of order vp, i.e. $\mathbf{I}_{vp}(\square)$ and $\mathbf{K}_{vp}(\square)$.

F. Parasitic Eddy-Current Losses

The average eddy-current losses in the conducting regions, over an electrical cycle $T = 2\pi/\omega_0$, can be calculated from Poynting's theorem [9-12]:

$$\left\langle P_{\mathbf{k}}\right\rangle = \frac{p\cdot R_{\mathbf{k}}\cdot L_m}{\sigma_{\mathbf{k}}\cdot\mu_{\mathbf{k}}}\cdot\int_0^{2\pi/p}\Re_e\left\{J_{\mathbf{k}}^{z}\cdot B_{\mathbf{k}ri}^{\Theta\,*}\right\}_{r=R_{\mathbf{k}}}\cdot d\Theta_r\,, \tag{15}$$

where $R_{\mathbf{k}}$ is the radius of conducting regions (i.e. Region.II: R_m, and Region.III: R_{r2}), and L_m the axial length of PM.

By introducing the equations (10.a), (10.g), and (14) in the equation (15), the average eddy-current losses are defined in Region.III by

$$\left\langle P_{\mathbf{III}}\right\rangle = \Re_e\left\{\sum_{u=-\infty}^{+\infty}\sum_{v=-\infty}^{+\infty}\frac{(u+v)}{vp}\cdot\left|\underline{J_m}_{uv}\right|^2\cdot\underline{C_9}_{uv}\right\}, \tag{16.a}$$

and in Region.II by

$$\left\langle P_{\mathbf{II}}\right\rangle = \Re_e\left\{\sum_{u=-\infty}^{+\infty}\sum_{v=-\infty}^{+\infty}\frac{(u+v)}{vp}\cdot\left|\underline{J_m}_{uv}\right|^2\cdot\underline{C_{10}}_{uv}\right\} - \left\langle P_{\mathbf{III}}\right\rangle, \tag{16.b}$$

where $\underline{C_9}_{uv}$ and $\underline{C_{10}}_{uv}$ are the harmonic coefficients of losses in the two conducting regions, which are given in the Tab. I. It can be noted that the first term in the above expression corresponds to the average parasitic eddy-current losses in the turning parts, $\left\langle P_{\mathbf{tp}}\right\rangle$.

One can remark that, in the equations (16), these average eddy-current losses are proportional to the square of the current. The combinations of the time harmonic u and the spatial harmonic v for which $(u+v)=0$ are synchronous with the rotor, and, therefore, do not create eddy-current losses, but contribute to the generation of torque. In a Brushless SMPMM, combinations of time and spatial harmonic components for which $(u+v)=6,12,18,...,$ are not synchronous with the rotor, and, therefore, contribute to generation of the average eddy-current losses.

Table I
Main harmonic amplitudes, coefficients and adimensional ratios of AM.

Regions	*Components*	*The harmonic amplitudes of the time-varying armature reaction magnetic flux density vector*
I	Radial	$\underline{B^{r}_{\mathbf{I}ri}}_{uv} = -j\cdot\frac{k_s\cdot\mu_0\cdot\underline{J_m}_{uv}}{\underline{K_d}_{uv}}\cdot\underline{K^{+}_{nI}}_{uv}(r)$
	Tangential	$\underline{B^{\Theta}_{\mathbf{I}ri}}_{uv} = -\frac{k_s\cdot\mu_0\cdot\underline{J_m}_{uv}}{\underline{K_d}_{uv}}\cdot\underline{K^{-}_{nI}}_{uv}(r)$
II	Radial	$\underline{B^{r}_{\mathbf{II}ri}}_{uv} = -j\cdot\frac{2k_s\cdot\mu_{II}\cdot\underline{J_m}_{uv}}{\underline{K_d}_{uv}}\cdot r_I^{vp-k_s}\cdot\left[\underline{i^{+-}_{\mathbf{K}}}\cdot\mathbf{I}_{vp}\left(\underline{r_{II}}_{uv}(r)^{-1}\right)+\underline{i^{-+}_{\mathbf{I}}}\cdot\mathbf{K}_{vp}\left(\underline{r_{II}}_{uv}(r)^{-1}\right)\right]\cdot\underline{r_{II}}_{uv}(r)$
	Tangential	$\underline{B^{\Theta}_{\mathbf{II}ri}}_{uv} = -\frac{2k_s\cdot\mu_{II}\cdot\underline{J_m}_{uv}}{\underline{K_d}_{uv}}\cdot r_I^{vp-k_s}\cdot\left[\underline{i^{-+}_{\mathbf{I}}}\cdot\underline{h^{+}_{\mathbf{K}}}\left(\underline{r_{II}}_{uv}(r)^{-1}\right)-\underline{i^{+-}_{\mathbf{K}}}\cdot\underline{h^{-}_{\mathbf{I}}}\left(\underline{r_{II}}_{uv}(r)^{-1}\right)\right]$
III	Radial	$\underline{B^{r}_{\mathbf{III}ri}}_{uv} = -j\cdot\frac{2k_s\cdot\mu_0\cdot\underline{J_m}_{uv}}{\underline{K_d}_{uv}}\cdot r_I^{vp-k_s}\cdot\underline{C_7}\cdot\left[\mathbf{I}_{vp}\left(\underline{r_{III}}_{uv2}^{-1}\right)\cdot\mathbf{K}_{vp}\left(\underline{r_{III}}_{uv}(r)^{-1}\right)-\mathbf{K}_{vp}\left(\underline{r_{III}}_{uv2}^{-1}\right)\cdot\mathbf{I}_{vp}\left(\underline{r_{III}}_{uv}(r)^{-1}\right)\right]\cdot\underline{r_{III}}_{uv}(r)$
	Tangential	$\underline{B^{\Theta}_{\mathbf{III}ri}}_{uv} = -\frac{2k_s\cdot\mu_0\cdot\underline{J_m}_{uv}}{\underline{K_d}_{uv}}\cdot r_I^{vp-k_s}\cdot\underline{C_7}\cdot\left[\mathbf{K}_{vp}\left(\underline{r_{III}}_{uv2}^{-1}\right)\cdot\underline{h^{-}_{\mathbf{I}}}\left(\underline{r_{III}}_{uv}(r)^{-1}\right)+\mathbf{I}_{vp}\left(\underline{r_{III}}_{uv2}^{-1}\right)\cdot\underline{h^{+}_{\mathbf{K}}}\left(\underline{r_{III}}_{uv}(r)^{-1}\right)\right]$

Harmonic coefficients

$$\underline{K^{\pm}_{nI}}_{uv}(r)=\left[\underline{C_8^{+-}}\cdot\underline{r_{I_1}}(r)^{(1+k_s)\cdot vp}\pm\underline{C_8^{-+}}\cdot\underline{r_{I_1}}(r)^{(1-k_s)\cdot vp}\right]\cdot\underline{r_{I_2}}(r)^{vp-k_s}$$

$$\underline{K_d}_{uv}=\underline{C_8^{+-}}\cdot r_I^{(1+k_s)\cdot vp}-\underline{C_8^{-+}}\cdot r_I^{(1-k_s)\cdot vp}$$

$$\underline{h^{\pm}_{\mathbf{I}/\mathbf{K}}}\left(\underline{x_{\mathbf{k}}}_{uv}\right)=\frac{1}{vp}\cdot\mathbf{I}/\mathbf{K}_{vp-1}\left(\underline{x_{\mathbf{k}}}_{uv}\right)\pm\frac{1}{\underline{x_{\mathbf{k}}}_{uv}}\cdot\mathbf{I}/\mathbf{K}_{vp}\left(\underline{x_{\mathbf{k}}}_{uv}\right)$$

$$\underline{i^{\pm\mp}_{\mathbf{I}/\mathbf{K}}}=\underline{h^{\pm}_{\mathbf{I}/\mathbf{K}}}\left(\underline{r_{II}}_{uv2}^{-1}\right)\cdot\underline{r_{III}}_{uv1}\cdot\underline{C_1}\mp\mathbf{I}/\mathbf{K}_{vp}\left(\underline{r_{II}}_{uv2}^{-1}\right)\cdot\underline{r_{II}}_{uv2}\cdot\underline{C_2}$$

$$\underline{C_1}=\nu_{rII}\cdot\left[\mathbf{I}_{vp}\left(\underline{r_{III}}_{uv2}^{-1}\right)\cdot\mathbf{K}_{vp}\left(\underline{r_{III}}_{uv1}^{-1}\right)-\mathbf{I}_{vp}\left(\underline{r_{III}}_{uv1}^{-1}\right)\cdot\mathbf{K}_{vp}\left(\underline{r_{III}}_{uv2}^{-1}\right)\right]$$

$$\underline{C_7}=\underline{r_{II}}_{uv2}\cdot\left[\mathbf{K}_{vp}\left(\underline{r_{II}}_{uv2}^{-1}\right)\cdot\underline{h^{-}_{\mathbf{I}}}\left(\underline{r_{II}}_{uv2}^{-1}\right)+\mathbf{I}_{vp}\left(\underline{r_{II}}_{uv2}^{-1}\right)\cdot\underline{h^{+}_{\mathbf{K}}}\left(\underline{r_{II}}_{uv2}^{-1}\right)\right]$$

$$\underline{C_2}=\nu_{rIII}\cdot\left[\underline{h^{-}_{\mathbf{I}}}\left(\underline{r_{III}}_{uv1}^{-1}\right)\cdot\mathbf{K}_{vp}\left(\underline{r_{III}}_{uv2}^{-1}\right)+\mathbf{I}_{vp}\left(\underline{r_{III}}_{uv2}^{-1}\right)\cdot\underline{h^{+}_{\mathbf{K}}}\left(\underline{r_{III}}_{uv1}^{-1}\right)\right]$$

$$\underline{C_8^{\pm\mp}}=\underline{r_{III}}_{uv1}\cdot\underline{C_1}\cdot\underline{C_5^{\pm\mp}}+\underline{r_{II}}_{uv2}\cdot\underline{C_2}\cdot\underline{C_6^{\pm\mp}}$$

$$\underline{C_3^{\pm}}=\left(\mu_{rII}\pm1\right)\cdot\underline{r_{II}}_{uv1}\cdot\mathbf{K}_{vp}\left(\underline{r_{II}}_{uv1}^{-1}\right)\pm\frac{1}{vp}\cdot\mathbf{K}_{vp-1}\left(\underline{r_{II}}_{uv1}^{-1}\right)$$

$$\underline{C_9}=-8\,j\pi\cdot k_s\cdot\mu_{II}\cdot\omega_0\cdot L_m\cdot {R_{r2}}^2\cdot r_I^{2\cdot(vp-k_s)}\cdot\underline{r_{III}}_{uv1}\cdot\left|\frac{\underline{C_7}}{\underline{K_d}_{uv}}\right|^2\cdot\underline{C_1}\cdot\underline{C_2}^{*}$$

$$\underline{C_4^{\pm\mp}}=\left(\mu_{rII}\pm1\right)\cdot\underline{r_{II}}_{uv1}\cdot\mathbf{I}_{vp}\left(\underline{r_{II}}_{uv1}^{-1}\right)\mp\frac{1}{vp}\cdot\mathbf{I}_{vp-1}\left(\underline{r_{II}}_{uv1}^{-1}\right)$$

$$\underline{C_{10}}=-8\,j\pi\cdot k_s\cdot\mu_{II}\cdot\omega_0\cdot L_m\cdot {R_m}^2\cdot r_I^{2\cdot(vp-k_s)}\cdot\underline{r_{II}}_{uv1}\cdot\left|\frac{1}{\underline{K_d}_{uv}}\right|^2\cdot\underline{C_{11}}\cdot\underline{C_{12}}^{*}$$

$$\underline{C_5^{\pm\mp}}=\underline{h^{-}_{\mathbf{I}}}\left(\underline{r_{II}}_{uv2}^{-1}\right)\cdot\underline{C_3^{\pm}}+\underline{C_4^{\pm\mp}}\cdot\underline{h^{+}_{\mathbf{K}}}\left(\underline{r_{II}}_{uv2}^{-1}\right)$$

$$\underline{C_{11}}=\underline{i^{+-}_{\mathbf{K}}}\cdot\mathbf{I}_{vp}\left(\underline{r_{II}}_{uv1}^{-1}\right)+\underline{i^{-+}_{\mathbf{I}}}\cdot\mathbf{K}_{vp}\left(\underline{r_{II}}_{uv1}^{-1}\right)$$

$$\underline{C_6^{\pm\mp}}=\mathbf{I}_{vp}\left(\underline{r_{II}}_{uv2}^{-1}\right)\cdot\underline{C_3^{\pm}}-\underline{C_4^{\pm\mp}}\cdot\mathbf{K}_{vp}\left(\underline{r_{II}}_{uv2}^{-1}\right)$$

$$\underline{C_{12}}=\underline{i^{-+}_{\mathbf{I}}}\cdot\underline{h^{+}_{\mathbf{K}}}\left(\underline{r_{II}}_{uv1}^{-1}\right)-\underline{i^{+-}_{\mathbf{K}}}\cdot\underline{h^{-}_{\mathbf{I}}}\left(\underline{r_{II}}_{uv1}^{-1}\right)$$

Regions	*Adimensional ratios*
I	$r_I=r_{I_1}(r)\cdot r_{I_2}(r)=\left(R_m/r\right)^{k_s}\cdot\left(r/R'_s\right)^{k_s}=\left(R_m/R'_s\right)^{k_s}$
II	$\underline{r_{II}}_{uv}(r)=\underline{\delta_{II}}_{uv}/r$, $\underline{r_{II}}_{uv1}=\underline{\delta_{II}}_{uv}/R_m$, and $\underline{r_{II}}_{uv2}=\underline{\delta_{II}}_{uv}/R_{r2}$
III	$\underline{r_{III}}_{uv}(r)=\underline{\delta_{III}}_{uv}/r$, $\underline{r_{III}}_{uv1}=\underline{\delta_{III}}_{uv}/R_{r2}$, and $\underline{r_{III}}_{uv2}=\underline{\delta_{III}}_{uv}/R_{r1}$

3. COMPARISON WITH FINITE ELEMENT SIMULATIONS

The developed AM has been applied to various motor topologies. We give the results of a 2-pole, 10000 rpm, 500 W, 3-phase, Brushless motor with an internal rotor topology whose main parameters are given in Tab. II. The machine was surface-mounted, parallel magnetised sintered Nd-Fe-B magnets, and had a two slot/pole/phase overlapping stator winding.

Fig. 2. shows the analytical and numerical eddy-current losses in two conducting regions versus the time for an operating speed of 10000 rpm and for sinusoidal phase current waveforms, with ($I = 3.343$ A RMS). One can remark that the average eddy-current losses in Region.III are negligible in comparison with the losses in Region.II and that the agreement of the results of both analytical and numerical calculations is quite good (less than 2 %).

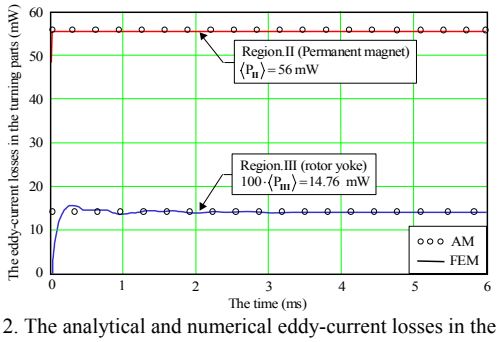

Fig. 2. The analytical and numerical eddy-current losses in the two conducting regions.

Fig. 3. plots the losses in load motor mode versus the machine's rotational speed for the current level, $I = 3.343$ A RMS. The average eddy-current losses are given for the whole rotor (i.e. in the turning parts) with a slotted stator and a slotless stator. It can be observed that these losses are proportional to the square of the speed, due to the increased of the skin effect. One could also note that the losses resulting from stator slotting permeance harmonics are negligible because of the low ratios of b_0/τ_t .

4. CONCLUSION

A 2-D AM in polar co-ordinates has been developed to estimate the parasitic eddy-current losses in the turning parts for high-speed SMPMM having either internal or external rotor topologies and overlapping stator windings. This model accounts for curvature, time and space MMF harmonics, and effect of the eddy-current reaction field, but, it neglects the effect of the slotting. The accuracy of the AM has been proved by comparison with FEM simulations. A possible outlook of the work is now to develop an AM taking into account the slot effect.

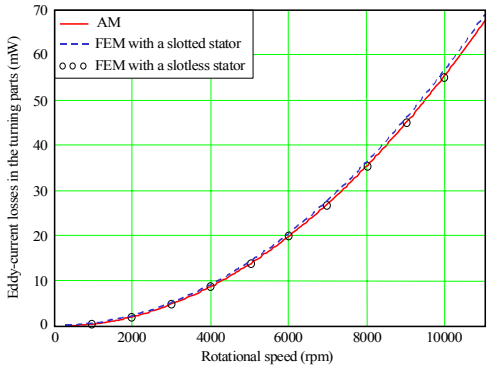

Fig. 3. Losses in load motor mode versus motor speed in the turning parts.

Table II
Main parameters of 2-pole, 10000 rpm, 500 W, 3-phases, Brushless SMPMM with internal rotor

Parameters	Values
Axial length of PM, L_m	45 mm
Carter's coefficient, K_c	1.011
Ratios of b_0/τ_t	0.2
Ratios of R_m/R'_s , R_{r2}/R_m , R_{r1}/R_{r2}	0.947 , 0.737 , 0
Conductivity of Region.II, σ_{II}	$0.694\times10^6\ (\Omega\cdot m)^{-1}$
Conductivity of Region.III, σ_{III}	$4.227\times10^6\ (\Omega\cdot m)^{-1}$
Relative permeability of Region.II, μ_{rII}	1.029
Relative permeability of Region.II, μ_{rIII}	1123
Number of series turns per phase, N	48
Number of layers, N_c	2
Span of tooth inclination, y_i	0
winding pitch (shortening step), y_{wp}	5/6

REFERENCES

[1] I.E.D. Pickup, D. Tipping, D.E. Hesmondhalgh, and B.A.T. Al Zahawi, "A 250,000 rpm drilling spindle using a permanent magnet motor", in *Proc. Int. Conf. on Electr. Mach.*, Vol. 2/3, 1996, pp. 337-342.

[2] K.J. Binns, P.J.G. Lisboa, and M.S.N. Al-din, "The use of canned rotors in high speed permanent magnet machines", *in Proc. Int. Conf. on Electr. Mach. and Drives*, No. 341, 1991, pp. 21-25.

[3] N. Boules, "Impact of slot harmonics on losses of high-speed permanent magnet machines with a magnet retaining ring", *Electr. Mach. Electromech.*, Vol. 6, 1981, pp. 527-539.

[4] B.C. Mecrow, A.G. Jack, and J.M. Mastermann, "Determination of rotor eddy current losses in permanent magnet machines", in *Proc. Int. Conf. on Electr. Mach. and Drives*, 1993, pp. 299-304.

[5] K. Ng, Z.Q. Zhu, and D. Howe, "Open-circuit field distribution in a brushless motor with diametrically magnetised PM rotor, accounting for slotting and eddy current effects", *IEEE Trans. on Magn.*, Vol. 32, No. 5, 1996, pp. 5070-5072.

[6] K. Yoshida, K. Kesmaru, and Y. Hita, "Eddy currents analysis of surface-mounted PMSM by finite element method", *in Proc. Int. Conf. on Electr. Mach.*, Vol. 3/3, 1998, pp. 1821-1825.

[7] K. Atallah, D. Howe, P.H. Mellor, and D.A. Stone, "Rotor loss in permanent magnet brushless AC machines", *IEEE Trans. Ind. Appl.*, Vol. 36, No. 6, 2000, pp. 1612-1618.

[8] Z.Q. Zhu, K. Ng, N. Schofield, and D. Howe, "Analytical prediction of rotor eddy current loss in Brushless machines equipped with surface-mounted permanent magnets, part I: magnetostatic field model", *in Proc. Int. Conf. on Electr. Mach. and Syst.*, Vol. 2, 2001, pp. 806-809.

[9] F. Deng, "Commutation-caused-eddy-current losses in permanent-magnet Brushless DC motors", *IEEE Trans. on Magn.*, Vol. 33, No. 5, 1997, pp. 4310-4318.

[10] F. Deng, "Improved analytical modeling of commutation losses including space harmonic effects in permanent magnet Brushless DC motors", *in Proc. Ind. Appl.*, Vol. 1, 1998, pp. 380-386.

[11] Z.Q. Zhu, K. Ng, N. Schofield, and D. Howe, "Analytical prediction of rotor eddy current loss in Brushless machines equipped with surface-mounted permanent magnet, part II: accounting for eddy current reaction field", *in Proc. Int. Conf. on Electr. Mach. and Syst.*, Vol. 2, 2001, pp. 810-813.

[12] F. Deng, "Analytical modeling of eddy-current losses caused by pulse-width-modulation switching in permanent-magnet Brushless DC motors", *IEEE Trans. on Magn.*, Vol. 34, No. 5, 1998, pp. 3728-3726.

[13] Flux2D, "Notice d'utilisation générale", Version 7.50., Cedrat S.A Electrical Engineering, 10 Chemin de pré carré, Zirst, 38246 MEYLAN Cedex-FRANCE.

[14] J. Saint-Michel, "Bobinage des machines tournantes à courant alternatifs", *Techniques de l'Ingénieur*, Traité de Génie Électrique, D 3420, 2001, pp. 01-24.

[15] Q. Gu and H. Gao, "Effect of slotting in PM electrical machines", *Elect. Mach. Power Syst.*, Vol. 10, No. 2, 1985, pp. 273-284.